

## Optical Precursor with Four-Wave Mixing and Storage Based on a Cold-Atom Ensemble

Dong-Sheng Ding,<sup>1,2</sup> Yun Kun Jiang,<sup>3</sup> Wei Zhang,<sup>1,2</sup> Zhi-Yuan Zhou,<sup>1,2</sup> Bao-Sen Shi,<sup>1,2,\*</sup> and Guang-Can Guo<sup>1,2</sup>

<sup>1</sup>Key Laboratory of Quantum Information, University of Science and Technology of China, Hefei 230026, China

<sup>2</sup>Synergetic Innovation Center of Quantum Information & Quantum Physics,  
University of Science and Technology of China, Hefei, Anhui 230026, China

<sup>3</sup>College of Physics and Information Engineering, Fuzhou University, Fuzhou 350002, People's Republic of China

(Received 12 November 2014; published 3 March 2015)

We observed optical precursors in four-wave mixing based on a cold-atom gas. Optical precursors appear at the edges of pulses of the generated optical field, and propagate through the atomic medium without absorption. Theoretical analysis suggests that these precursors correspond to high-frequency components of the signal pulse, which means the atoms cannot respond quickly to rapid changes in the electromagnetic field. In contrast, the low-frequency signal components are absorbed by the atoms during transmission. We also showed experimentally that the backward precursor can be stored using a Raman transition of the atomic ensemble and retrieved later.

DOI: 10.1103/PhysRevLett.114.093601

PACS numbers: 42.50.Md, 32.80.Qk, 42.25.Bs, 42.50.Gy

Optical precursors are interesting phenomena that arise from the edge of a classical electromagnetic field pulse and go out directly without absorption when they propagate through an absorbing medium [1,2]. This phenomenon has been studied in the  $\gamma$ -ray [3], microwave [4], and optical regimes [5–8], and in electromagnetically induced transparency (EIT) media [9–15]. The underlying physical mechanism is that the response of the medium lags behind that of the high-frequency components of the electromagnetic field. In EIT media, Du *et al.* [9,12–15] experimentally observed the precursor for both the classical electromagnetic field [12] and that for a single photon [14], in which the low-frequency components of the input signal field are delayed by the atoms and the high-frequency components pass through the atoms without any delay.

No experimental demonstrations exist of optical precursors in a nonlinear optical process, such as the four-wave mixing (FWM) process. FWM has been studied by many groups in atomic systems with double lambda [16–19], ladder, or diamond-type configurations [20–24]. FWM is usually used for frequency conversion of photons or optical pulses. In this Letter, we report on the observation of an interesting optical filtering effect in a FWM process using an inverted Y-type configuration in cold atoms; specifically, optical precursors of a generated signal field appear. We theoretically found and experimentally proved that if the edge of an input pulse is very steep, then the optical precursors are generated more easily. In addition, we experimentally achieved storage of the backward precursor, which showed that off-resonance storage can be performed even when the optical density is low. In the nonlinear optics and optical storage fields, our results offer a new understanding in that they demonstrate that the response rate of atoms in a nonlinear process is always faster than that of atoms in a linear process in an ensemble medium.

The inverted Y-type configuration used in our experiment [Fig. 1(a)] consists of the doubly degenerate ground states  $|1\rangle$  and  $|2\rangle$  ( $5S_{1/2}$   $F=3$ ), one intermediate state  $|3\rangle$  ( $5P_{1/2}$   $F'=2$ , decay rate  $\gamma$ ), and one upper state  $|4\rangle$  ( $4D_{3/2}$   $F''=2$ , decay rate  $\Gamma$ ). The atomic transition between the ground state and the intermediate state matches the  $D_1$  line of rubidium-85 ( $^{85}\text{Rb}$ ), and the transition between the intermediate state and the upper state is driven by another laser at a wavelength of 1475.6 nm. We experimentally generated a new electromagnetic field at 795 nm by combining the coupling laser, pump 1, and probe fields via a noncollinear FWM configuration.

In brief, the experimental setup [Fig. 1(b)] uses a continuous wave (cw) laser beam with a wavelength of 795 nm from an external-cavity diode laser (DL100, Toptica, Gräfelfing, Germany) impinging on a two-dimensional magneto-optical trap as the coupling light. A cw laser beam at 1475.6 nm from another external-cavity diode laser (DL100, Prodesign, Toptica) was split into two beams using a beam splitter to prepare the pump and probe beams. These fields were horizontally linearly polarized and

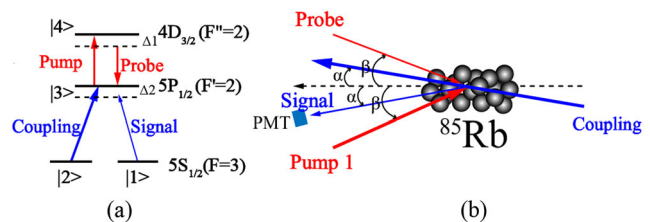


FIG. 1 (color online). (a) Experimental energy level diagram showing doubly degenerate ground states corresponding to sublevels ( $5S_{1/2}$   $F=3$ ), which includes levels from  $m_F = -3$  to  $m_F = 3$ . The atoms are polarized along the direction of the coupling laser. The pump and coupling beams are on resonance. (b) Simplified experimental setup. The angles  $\alpha \approx 1^\circ$  and  $\beta \approx 2^\circ$ .

modulated by two acousto-optic modulators. The coupling field acted as the pumping light in the FWM process and as the control light in the storage process. The probe field was focused using a lens with a focal length of 500 mm; the Fourier plane of the lens was at the center of the atomic ensemble. The generated signal field, which was focused by another lens, was collected using a multimode fiber, and was monitored using a photomultiplier tube (PMT) (H10721, Hamamatsu Photonics, Hamamatsu, Japan).

Before presenting our experimental results, we first present a simplified theoretical description of our system. According to Ref. [16], we derived steady-state solutions for the density matrix, neglecting terms that were higher than first order in the signal field, and obtained the susceptibility of the signal field  $\chi^{(3)}$  using  $P_s = N\mu_{31}\rho_{31} = \epsilon_0\chi^{(3)}E_{pr}^*$ , where  $N$  is the effective density of the atoms;  $\mu_{31}$  and  $\rho_{31}$  are the dipole element, and the density matrix element of the atomic transition  $|3\rangle \rightarrow |1\rangle$ , respectively;  $\epsilon_0$  is the permittivity of a vacuum, and  $E_{pr}^*$  is the conjugate of the probe field. Therefore,

$$\chi^{(3)} = \frac{N\mu_{31}\mu_{43}}{i\epsilon_0\hbar} \frac{A_1\Omega_P\Omega_C}{A_2(\Gamma_1 + \Gamma) + A_3\Gamma_1}, \quad (1)$$

where  $A_1$ ,  $A_2$ , and  $A_3$  are complex coefficients, which are functions of the pump and coupling Rabi frequencies,  $\Omega_P$  and  $\Omega_C$ , respectively, the decay rates  $\gamma$  and  $\Gamma$ , and the probe field detuning parameter  $\Delta_1$ . The coefficient  $\Gamma_1$  satisfies  $\Gamma_1 = \gamma - i\Delta_2$ , where the parameter  $\Delta_2$  determines the detuning between the atomic transition  $|3\rangle \rightarrow |1\rangle$  and the signal field. We plotted the susceptibility  $\chi^{(3)}$  against the detuning  $\Delta_2$ , while assuming that  $\Delta_1 = 0$  [red line in Fig. 2(a)]. The bandwidth of the FWM process was  $\sim 10$  MHz. The transmission of the signal field [blue line in Fig. 2(a)] takes the form  $E_s \propto E^{-\alpha/[1+(\Delta_2/\gamma)^2]}$ , where the parameter  $\alpha$  characterizes the optical density of the atoms. We chose  $\Delta_1 = -\Delta_2$  to make the two-photon transition towards the upper level resonant. We then plotted the spectrum of  $\chi^{(3)}$  [Fig. 2(b)], which is broader than the absorption spectrum of the probe.

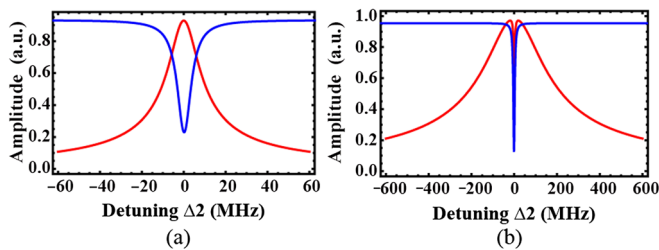


FIG. 2 (color online). (a) Spectra of the susceptibility  $\chi^{(3)}$  (red line) for a fixed probe detuning  $\Delta_1 = 0$  and of the corresponding transmission from the atoms (blue line) when  $\alpha = 1$ . (b) Spectrum of  $\chi^{(3)}$  (red line) for a varying probe detuning  $\Delta_1 = -\Delta_2$ . The blue line indicates the absorption spectrum of the probe.

Next, we used a square-shaped pulse as an input probe [Fig. 3(a)]; the edge gradient of this pulse, which is characterized by the coefficient  $k$ , takes the form  $E_s \propto E^{-k(t-t_0)^2}$ . The Fourier transformation of this pulse is given in Fig. 3(b). By filtering using the atomic nonlinear susceptibility  $\chi^{(3)}$  and the transmission spectrum of Fig. 2(b), the spectrum of Fig. 3(b) becomes that of Fig. 3(c); the low-frequency part of the signal is filtered while the high-frequency part is enhanced. The spectrum that was obtained was the result of a nonlinear process and an atomic absorption process. Figure 3(d) is the inverse Fourier transformation of Fig. 3(c), and corresponds to the output signal pulse. From this result, we see that the high-frequency components of the input probe are converted into a FWM field and transmitted from the atoms with little absorption. This is because the nonlinear spectrum of  $\chi^{(3)}$  is broader than the linear absorption spectrum of the atoms. The atoms respond too late to the high-frequency components of the FWM field, and thus we are able to see the optical precursor of the generated signal pulse, i.e., the generated signal field is always composed of those signal components from the FWM process that generate no absorption response from the atoms.

We also varied the coefficient  $k$  by considering an input half-Gaussian pulse, which corresponded directly to the quantity of high-frequency components of the signal field that were generated. The simulated results are shown in Fig. 4. In practical simulations, the timing width of the pulse  $\Delta t$  was changed using an arbitrary function generator, AFG3252. In Fig. 4(a), the peak height decreases with decreasing  $\Delta t$ . This point fully illustrates the fact that the high-frequency components of the signal field pass through the atoms more easily. To show this behavior clearly, we set

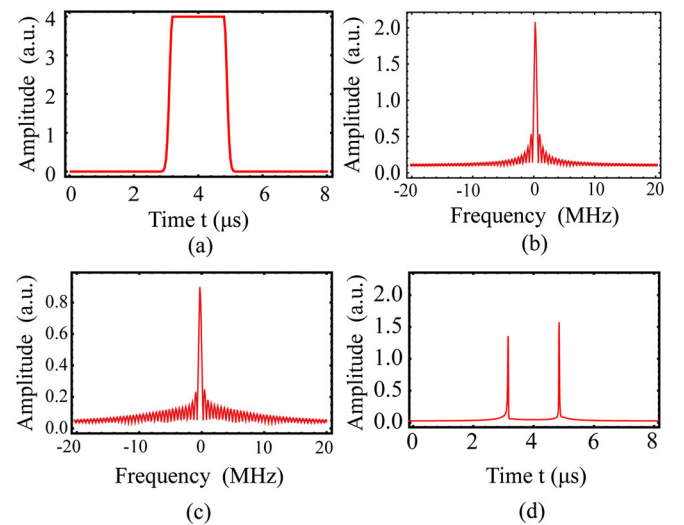


FIG. 3 (color online). (a) Square pulse of the input probe, and (b) its Fourier transform; (c) filtering spectrum produced through interactions with atoms, and (d) its inverse Fourier transform.

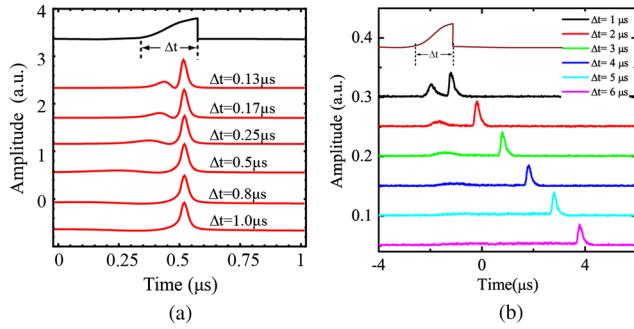


FIG. 4 (color online). Signal amplitudes of (a) different theoretical output pulses of the signal field vs the input half Gaussian shaped pulse with different pulse widths  $\Delta t$ , and (b) the experimentally generated signal fields for different periods of the half Gaussian pulse of 1–6  $\mu\text{s}$ . The powers of the probe, pump, and coupling were 0.45, 2.8, and 0.5 mW, respectively.

$\alpha = 0.01$ . For high values of  $\alpha$ , this filtering effect also appeared (see the experiment below).

We first performed nonlinear FWM using the experimental setup shown in Fig. 1(b). A cigar-shaped atomic cloud [25] was formed as the nonlinear medium. We used a PMT to monitor the generated signal field. The result (the black line in Fig. 5) shows that two optical precursors appeared at the leading and trailing edges. The interval between these precursors is composed of low-frequency components that are strongly absorbed by the atoms. As stated previously, the optical precursors appear because the nonlinear FWM spectrum is broader than the atomic adsorption bandwidth, and this results in the output of the high-frequency components of the signal field.

When we turned the coupling and pump fields off simultaneously, the back optical precursor disappeared,

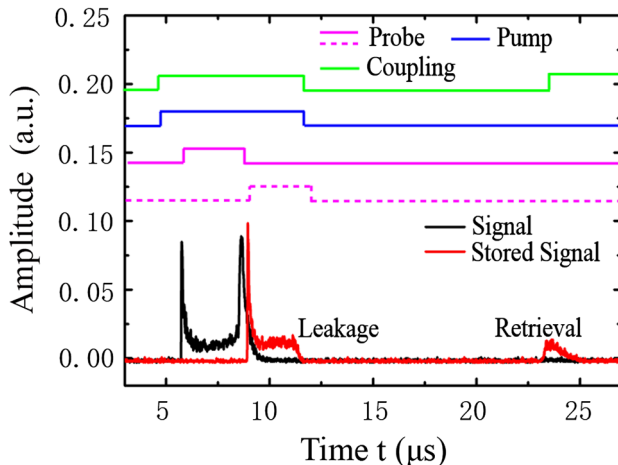


FIG. 5 (color online). Generated signal (black line) and leaked and retrieved signal (red line). The storage time was approximately 12  $\mu\text{s}$ . The timing sequences of the coupling (green), pump (blue), and probe (purple) fields are given in the upper half of the figure. The dotted purple line indicates the timing sequence of the pump and probe fields for the purpose of storing the signal.

(the red line in Fig. 5). The FWM signal was then retrieved by switching the coupling field back on. In this process, the atomic coherence state  $\rho_{12}(t)$  was prepared, and resulted in a memorizing signal field composed of a spin wave of atoms. In addition, if we used a coupling laser with detuning of  $-20$  MHz on the atomic transition  $|3\rangle \rightarrow |1\rangle$ , the optical precursors no longer appeared. This is because the signal field spectrum and the absorption spectrum of the atoms did not overlap.

In addition, we used a half Gaussian pulse as a probe pulse. As a result [see Fig. 6(a)], the precursor appeared at the steep edge of the pulse, and no precursor was observed at the shallow edge. At the same time, we varied the width of the half Gaussian pulse to check the relationship between the peak intensity and the steepness of the pulse edge. The results [see Fig. 4(b)] show an optical precursor at the steep edge but none at the shallow edge. These procedures demonstrate that the low-frequency components of the

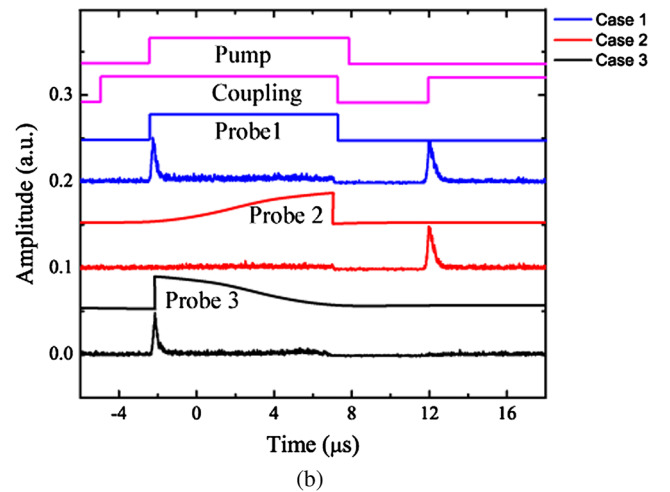
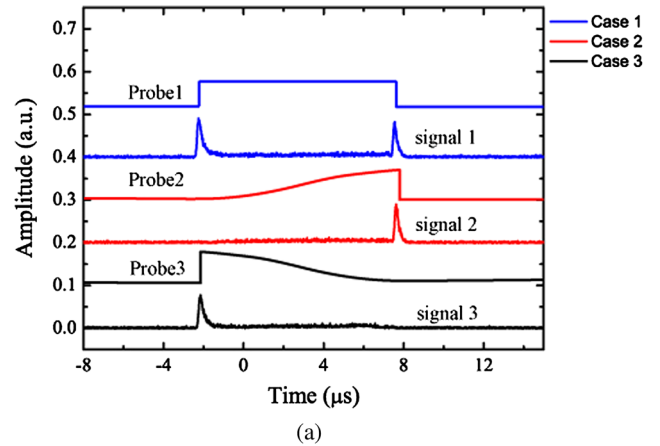


FIG. 6 (color online). (a) Amplitudes of generated signal fields vs different probe signal shapes. (b) Storage of the signal field vs differently shaped input probe signals. Case 1 was a square-shaped pulse; case 2 and case 3 corresponded to half Gaussian pulses. The powers of the probe, pump, and coupling are 0.45, 2.8, and 0.5 mW, respectively.

pulse edge were absorbed while the high-frequency components passed through the atoms. The experimental results are in accordance with previous theoretical explanations.

We tried to store the generated optical precursors; the results are shown in Fig. 6(b). Cases 1 and 2 clearly show that the generated backward precursor of the signal could be stored and retrieved later. In case 3, no signal storage was possible because there were no high-frequency components from the backward edge. Our results also supported the observations in Refs. [12,14] that if the frequency broadening of the pulse edge is greater than the bandwidth of the storage, no storage or delay of the narrow pulse is observed.

The work in Ref. [26] described a nonlinear optical spectrum filtering effect in a double FWM process, where two signal fields could be generated under the conditions for near two-photon resonance and where the single-photon detuning exceeded the absorption bandwidth of the cold atoms. Another point of note is that off-resonance storage in the FWM process was achieved in our system. This result was consistent with work reported in Refs. [27,28], where Raman quantum memory storage was performed under low optical depth conditions. In these studies, the storage bandwidth was broader than the absorption bandwidth of the cold atoms. Indeed, if the detuning of the single photon was too large, then the prepared signal could not be stored, in accordance with Ref. [29]. In Ref. [28], single photons with detuning of 200 MHz under conditions of the system's maximum limit were stored and retrieved, showing the maximum bandwidth for the nonlinear response of the medium.

In this study, we observed a filtering effect in the FWM process based on an inverted-Y-type atomic configuration. We theoretically analyzed and experimentally studied the bandwidth relationship between the input probe and the generated signal. We concluded that the high-frequency components of the edge pulse of the generated signal field propagated directly through the medium without absorption while the low-frequency components were absorbed. We also observed the storage of the backward optical precursor and its retrieval using a Raman transition. Our results are important for the fields of nonlinear optics and optical storage and help to provide a deeper understanding of the interactions between light and matter.

The authors would like to thank Professor Sheng-Wang Du for useful discussions. This work was supported by the National Fundamental Research Program of China (Grant No. 2 011CBA00200), the National Natural Science Foundation of China (Grants No. 11174271, No. 61275115, and No. 61435011), the Youth Innovation Fund from USTC (Grant No. ZC 9850320804), and the Innovation Fund from CAS.

D.-S. Ding and Y.-K. Jiang contributed equally to this work.

\*Corresponding author.

drshi@ustc.edu.cn

- [1] A. Sommerfeld, *Ann. Phys. (Berlin)* **349**, 177 (1914).
- [2] L. Brillouin, *Ann. Phys. (Berlin)* **349**, 203 (1914).
- [3] F. Lynch, R. Holland, and M. Hamermesh, *Phys. Rev.* **120**, 513 (1960).
- [4] P. Pleshko and I. Palocz, *Phys. Rev. Lett.* **22**, 1201 (1969).
- [5] J. Aaviksoo, J. Lippmaa, and J. Kuhl, *J. Opt. Soc. Am. B* **5**, 1631 (1988).
- [6] J. Aaviksoo, J. Kuhl, and K. Ploog, *Phys. Rev. A* **44**, R5353 (1991).
- [7] S.-H. Choi and U. L. Österberg, *Phys. Rev. Lett.* **92**, 193903 (2004).
- [8] H. Jeong and U. L. Österberg, *Phys. Rev. A* **77**, 021803(R) (2008).
- [9] H. Jeong and S. Du, *Phys. Rev. A* **79**, 011802(R) (2009).
- [10] W. R. LeFew, S. Venakides, and D. J. Gauthier, *Phys. Rev. A* **79**, 063842 (2009).
- [11] B. Macke and B. Ségard, *Phys. Rev. A* **80**, 011803(R) (2009).
- [12] D. Wei, J. F. Chen, M. M. T. Loy, G. K. L. Wong, and S. Du, *Phys. Rev. Lett.* **103**, 093602 (2009).
- [13] J. F. Chen, H. Jeong, L. Feng, M. M. T. Loy, G. K. L. Wong, and S. Du, *Phys. Rev. Lett.* **104**, 223602 (2010).
- [14] S. Zhang, J. F. Chen, C. Liu, M. M. T. Loy, G. K. L. Wong, and S. Du, *Phys. Rev. Lett.* **106**, 243602 (2011).
- [15] S. Du, C. Belthangady, P. Kolchin, G. Y. Yin, and S. E. Harris, *Opt. Lett.* **33**, 2149 (2008).
- [16] M. D. Lukin, P. R. Hemmer, and M. O. Scully, *Adv. At. Mol. Opt. Phys.* **42**, 347 (2000).
- [17] M. D. Lukin, P. Hemmer, M. Loeffler, and M. O. Scully, *Phys. Rev. Lett.* **81**, 2675 (1998).
- [18] P. R. Hemmer, D. P. Katz, J. Donoghue, M. Cronin-Golomb, M. S. Shahriar, and P. Kumar, *Opt. Lett.* **20**, 982 (1995).
- [19] A. J. Merriam, S. J. Sharpe, H. Xia, D. Manuszak, G. Y. Yin, and S. E. Harris, *Opt. Lett.* **24**, 625 (1999).
- [20] A. G. Radnaev, Y. O. Dudin, R. Zhao, H. H. Jen, S. D. Jenkins, A. Kuzmich, and T. A. B. Kennedy, *Nat. Phys.* **6**, 894 (2010).
- [21] P. S. Hsu, A. K. Patnaik, and G. R. Weich, *Opt. Lett.* **33**, 381 (2008).
- [22] R. T. Willis, F. E. Becerra, L. A. Orozco, and S. L. Rolston, *Phys. Rev. A* **79**, 033814 (2009).
- [23] D.-S. Ding, Z.-Y. Zhou, B.-S. Shi, X.-B. Zou, and G.-C. Guo, *Phys. Rev. A* **85**, 053815 (2012).
- [24] A. Gogyan, *Phys. Rev. A* **81**, 024304 (2010).
- [25] Y. Liu, J.-H. Wu, B.-S. Shi, and G.-C. Guo, *Chin. Phys. Lett.* **29**, 024205 (2012).
- [26] Y. Liu, J. Wu, D. Ding, B. Shi, and G. Guo, *New J. Phys.* **14**, 073047 (2012).
- [27] D.-S. Ding, W. Zhang, Z.-Y. Zhou, S. Shi, G.-Y. Xiang, X.-S. Wang, Y.-K. Jiang, B.-S. Shi, and G.-C. Guo, *Phys. Rev. Lett.* **114**, 050502 (2015).
- [28] D.-S. Ding, W. Zhang, Z.-Y. Zhou, S. Shi, B.-S. Shi, and G.-C. Guo, *arXiv:1410.7101*.
- [29] J. H. Wu, D. S. Ding, Y. Liu, Z. Y. Zhou, B. S. Shi, X. B. Zou, and G. C. Guo, *Phys. Rev. A* **87**, 013845 (2013).